Programmable Group-Delay Module Using Binary Polarization Switching

Lianshan Yan, *Student Member, IEEE, Student Member, OSA*, C. Yeh, G. Yang, L. Lin, Z. Chen, Y. Q. Shi, Alan Eli Willner, *Senior Member, IEEE, Fellow, OSA*, and X. Steve Yao

***Abstract*—We demonstrate the first programmable group-delay module based on polarization switching. With a unique binary tuning mechanism, the device can generate any differential group delay value from −45 to +45 ps with a resolution of 1.40 ps, or any true-time-delay value from 0 to 45 ps with a resolution of 0.7 ps. The delay varying speeds for both applications are under 1 ms and can be as fast as 0.1 ms. We evaluate both the dynamic and static performances of the device while paying special attention to its dynamic figures of merit for polarization-mode dispersion emulation and compensation applications. Our experiment shows that the device exhibits a negligible transient-effect induced power penalty ($<$ 0.2 dB) in a 10-Gb/s nonreturn-to-zero system.**

***Index Terms*—Differential group delay (DGD), optical communications, optical polarization, polarization-mode dispersion (PMD), time delay, true time delay (TTD).**

I. Introduction

DELAY GENERATION is an important function that may be necessary for both optical and microwave communication systems. Optical delay lines, such as differential-group-delay (DGD) and true-time-delay (TTD) lines, are key elements in high-performance transmission systems and networks.

DGD is characterized as the relative delay time between two orthogonal polarization states. In a high-speed optical transmission system, the nonideal shape of the optical fiber core and mechanical stress on the fiber induce birefringence along the fiber and generate DGD, which, in turn, causes the annoying problem of polarization-mode dispersion (PMD) [1], [2]. In general, the DGD and the principal axes of the fiber link depend on the wavelength and fluctuate in time as a result of temperature variations and external constraints [3]. Consequently, the corresponding pulse broadening caused by the PMD is random, both as a function of wavelength at a given time and as a function of time at a given wavelength. Unlike the effects of chromatic dispersion and fiber nonlinearity, which are deterministic and stable in time, the PMD-induced penalty can be totally absent at a given moment and adversely large several days later, causing an unacceptable bit error rate (BER) for no apparent reason. To ensure an acceptable outage probability for a fiber-optic system, PMD compensation must be dynamic in nature and must be able to adapt to the random time variations. Therefore, the major challenges for combating the PMD effect include: 1) accurate and fast emulation of PMD statistics and 2) dynamic DGD generation for compensating the PMD produced in the fiber link.

Tunable DGD modules are highly desirable for both PMD emulation and compensation. As a PMD emulator, a tunable DGD module can provide a desired distribution mimicking the PMD fluctuation in a real fiber link within a short period of time and can be used to evaluate the performance of PMD compensators.

A typical first-order PMD compensator consists of a polarization controller followed by either a fixed or a variable DGD element. Variable DGD-based PMD compensators can reduce the risk of feedback loops being trapped in a locally optimized state and provide superior performance compared with fixed compensators [4]. In addition, in PMD compensators that use polarization scrambling at the transmitter to reduce the complexity and increase the stability of the feedback control, a variable DGD element is required in order to exactly cancel out the fiber's DGD [5]–[8]. As higher order PMD effects become more significant, variable DGD elements may be required for higher-order PMD compensation as well [9]–[14].

The previous approach toward making a variable DGD element introduces a relative delay between two orthogonal polarization components after physically separating them with a polarization beam splitter (PBS). The two polarization components are then recombined with a polarization beam combiner (PMC) [5], [15]. This kind of device always has a low tuning speed (sub-second), a large output polarization fluctuation, a large footprint, and poor control certainty due to mechanical motion.

In high-speed time-division-multiplexing (TDM) systems, a variable TTD (sometimes referred to as "group delay") module can be used to precisely position data in an assigned time slot at the transmission end and select a desired time slot at the receiving end [16], [17]. In a microwave photonics system, a high-speed TTD module is desirable to perform microwave signal processing and phased-array radar beam forming functions [18]–[20]. In these applications, a versatile TTD requires not only a large time delay ($\sim$ microsecond) for wide dynamic range but also a fine delay resolution (sub-picosecond) to ensure accuracy. Because such a large time delay interval can be achieved with the optical path length switching approach, a reliable fine delay often becomes a challenge in device design. Several approaches [18]–[20], such as wavelength switching,

Manuscript received September 18, 2002; revised April 14, 2003.

L. Yan is with the General Photonics Corporation, Chino, CA 91710 USA, and also with the Department of Electrical Engineering—Systems, University of Southern California, Los Angeles, CA 90089-2565 USA (e-mail: lianshay@usc.edu).

C. Yeh, G. Yang, L. Lin, Z. Chen, Y. Q. Shi, and X. S. Yao are with the General Photonics Corporation, Chino, CA 91710 USA (e-mail: syao@generalphotonics.com).

A. E. Willner is with the Department of Electrical Engineering—Systems, University of Southern California, Los Angeles, CA 90089-2565 USA.

Digital Object Identifier 10.1109/JLT.2003.814383

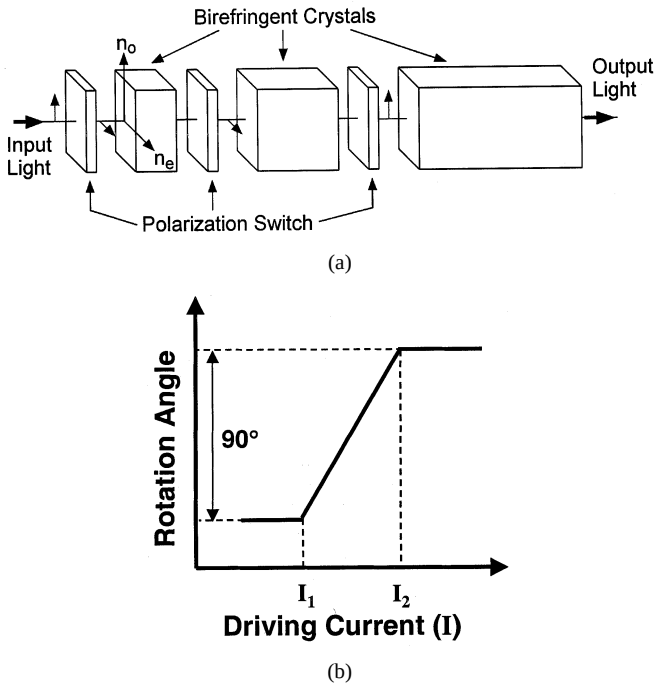

Fig. 1. (a) Illustration of a programmable DGD module based on polarization switching. (b) Typical response curve of a magnetooptic (MO) polarization switch.

have been proposed to achieve fine delay resolutions in a TTD. In 1994, Yao *et al.* first proposed photonic true time delay based on polarization switching [20] that can generate precisely controlled TTD and DGD; however, the concept was not demonstrated.

In this paper, we demonstrate a compact programmable photonic delay module based on the concept described in [20]. The module consists of six cascaded birefringent crystals separated by magnetooptic (MO) polarization switches. The lengths of the birefringent crystals are arranged in a binary power series, increasing by a factor of two in each section. The unique digital tuning mechanism ensures a precise and repeatable delay control to generate any DGD value from -45 to $+45$ ps in less than 1 ms with 1.40-ps resolution ($<$ 0.1-ps resolution can be readily achieved by design). When used as a TTD, the module can generate any TTD value from 0 to 45 ps with a resolution of 0.7 ps.

The operation principle is discussed in Section II, followed by basic static characterization in Section III. We show the first-order PMD emulation in Section IV, and system evaluation of its dynamic performance in Section V. Furthermore, Section VI lists some key applications of this module in fiber-optic and microwave photonics systems.

II. Operating Principle

The tunable DGD module employs a polarization-switching approach to generate different delays [19]. As shown in Fig. 1(a), the device is comprised of multiple switch/delay sections. Each switch/delay section consists of a birefringent crystal to generate a fixed amount of delay and an MO polarization switch. The MO switch is internally made using a driving coil and garnet crystals. The lengths of the birefringent crystals are arranged in a binary power series, increasing by a factor of two in each section. Such a binary arrangement requires a minimum number of crystal sections and results in the highest possible delay resolution. The typical response curve illustrating the binary nature of the MO switch is shown in Fig. 1(b). By driving the switch with current that is either less than the saturation current I_1 or greater than saturation the current I_2, 90° polarization rotation/switching is achieved. Thus, at any switch/delay section, the input polarized beam can be either switched along the slow or fast axes of the birefringent crystal, corresponding to a longer or shorter delay. The total delay is the summation of the delays in each crystal segment and can be varied by the MO polarization switches.

Assuming that the smallest birefringent crystal length is ℓ, we define a unit delay time $\delta\tau$ to represent the delay generated by the shortest delay section. The unit delay time can be expressed as

$$\delta\tau = \left|(n_e - n_o)\,\frac{\ell}{c}\right| \tag{1}$$

where n_o and n_e are the ordinary and extraordinary indexes of refraction, and c is the speed of light. Although the delay/switch sections can be placed in any order, we consider a case when the first bit (the least significant bit) in the switching command controls the shortest delay section and the last bit (the most significant bit) controls the longest delay section.

As mentioned in the introduction, the tunable delay module has two distinct applications: either providing variable DGD between two linear orthogonal polarization states or functioning as a photonic TTD by aligning the input state of polarization (SOP) to one of the eigen polarization axes of the crystal set.

When the module is utilized to produce variable time delay to orthogonal polarizations, i.e., tunable DGD, the focus is on the time delay between the two eigen-polarization states. In this situation, when the nth bit is switched from 0 to 1 state, the differential time delay of the nth section changes its sign. The total differential time delay for an arbitrary binary state becomes

$$\Delta\tau_d = -\delta\tau \sum_{n=1}^{6} (-1)^{b_n}\, 2^{n-1}. \tag{2}$$

where $b_n (= 0, 1)$ is the binary value of the nth bit, determined by the polarization switch associated with the nth bit. The delay resolution is twice the unit delay time, i.e., $2\delta\tau$, obtained by switching the least significant bit in (2). The DGD can be a negative number due to the sign flip of the delay time during switching. In a 6-bit module, a total of 64 DGD values (from $-63\delta\tau$ to $+63\delta\tau$) can be generated with a resolution of $2\delta\tau$.

When the variable delay module is used to provide TTD, the total absolute delay time $\Delta\tau_a$ at an arbitrary binary state is

$$\Delta\tau_a = \delta\tau \sum_{n=1}^{6} \left[1 - (-1)^{b_n}\right] 2^{n-2} + \tau_0 \tag{3}$$

where τ_0 is the constant bias time delay of the common optical path. Equation (3) shows that when the nth bit is switched from 0 (low) to 1 (high), the time delay of this section switches from the OFF state to the ON state. In a 6-bit module, 64 different delay combinations from $\Delta\tau_a = \tau_0$ to $\Delta\tau_a = 63\delta\tau + \tau_0$ can be generated with a delay resolution of $\delta\tau$ [as defined in (1)].

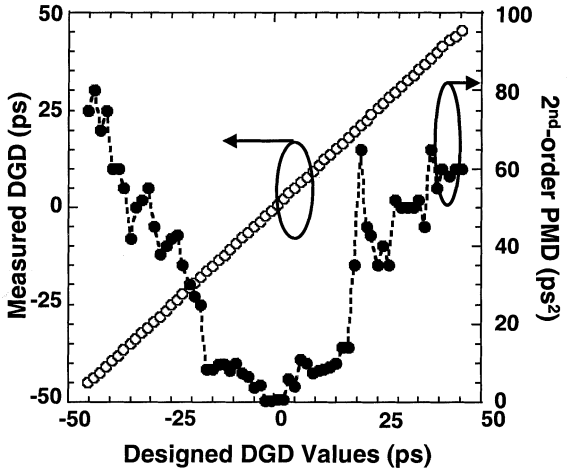

Fig. 2. Measured DGD and the second-order PMD as a function of designed DGD.

Based on the principle described in Fig. 1, we designed and fabricated a novel programmable delay module using six birefringent crystals (i.e., a 6-bit module) that can generate tunable DGD values from -45 to $+45$ ps with a resolution $(2\delta\tau)$ of 1.40 ps, or tunable TTD values from 0 to 45 ps with a resolution $(\delta\tau)$ of 0.7 ps. One of the most promising features of this module is the sub-millisecond switching speed desirable for PMD compensation, PMD emulation, as well as microwave signal processing applications.

III. Static Characteristics

A. DGD Characterization

We carefully measured the static characteristics of the tunable delay module for DGD generation. To verify the accuracy of generated DGD values of the module, we used a commercial PMD analyzer to measure both the DGD value and the second-order PMD at each logical DGD state. As shown in Fig. 2, the measured DGD values agree well with the designed DGD values, and each DGD value is exactly reproducible. Equally as important, the second-order PMD is very small, less than 85 ps^2, even at high values of DGD.

Insertion loss, wavelength-dependent loss (WDL), and polarization-dependent loss (PDL) are key figures of merit of any inline optical component. Fig. 3(a) shows the measured insertion loss as a function of wavelength across the C band (1535–1560 nm) using a broad-band amplified spontaneous emission (ASE) source, and Fig. 3(b) shows the measured PDL values for all designed DGD states. The insertion loss is $\sim$1.3 dB with a wavelength dependent variation of $<$0.15 dB. The PDL values range from 0.02 to $\sim$0.28 dB for all the DGD states.

B. TTD Measurement

When our tunable DGD module is utilized as a photonic TTD line, i.e., providing absolute delay, the minimum delay occurs when all b_n values are equal to zero (000 000 state) in (3), and the maximum delay occurs when all b_n values are equal to one (111 111 state). The total time delay and the delay resolution are proportional to the unit delay, and one can select appropriate birefringent crystals to achieve delay resolutions down to the femtosecond level for ideal fine delay tuning.

The absolute time delay or TTD is measured experimentally using a fiber-optic Mach–Zehnder interferometer, as illustrated in Fig. 4. Using a broad-band source centered at 1550 nm as the

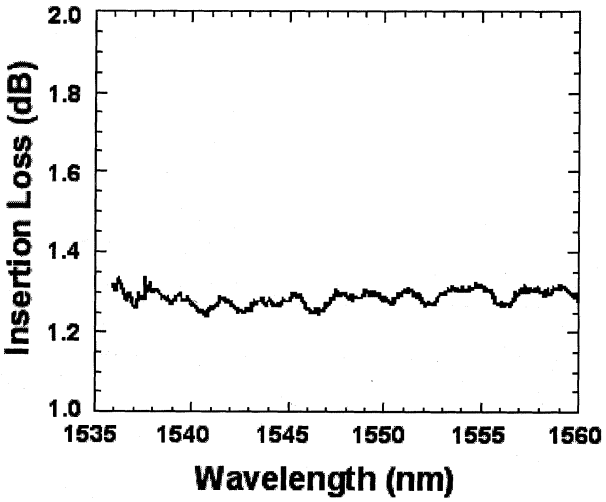

(a)

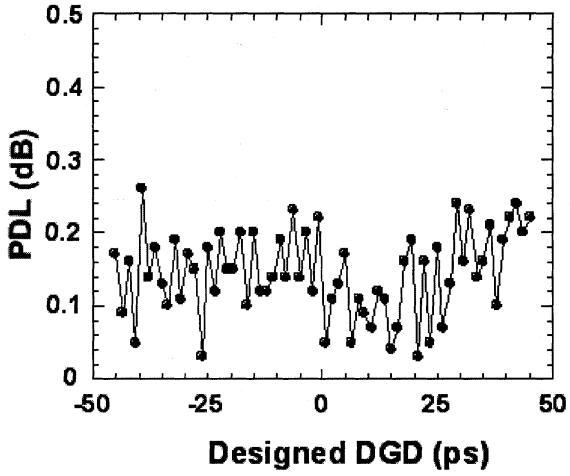

(b)

Fig. 3. (a) Insertion loss of the delay module as a function of wavelength (1535–1560 nm) at a typical DGD state (-40 ps). (b) Polarization-dependent loss (PDL) as a function of designed DGD values.

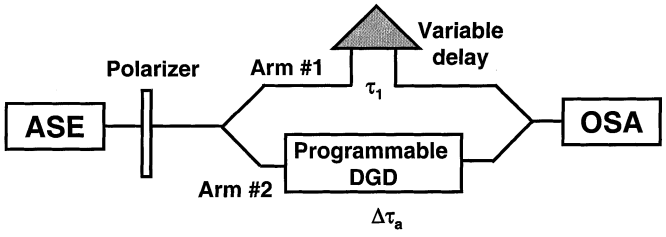

Fig. 4. TTD measurement setup using an ASE broad-band source. OSA: Optical spectrum analyzer.

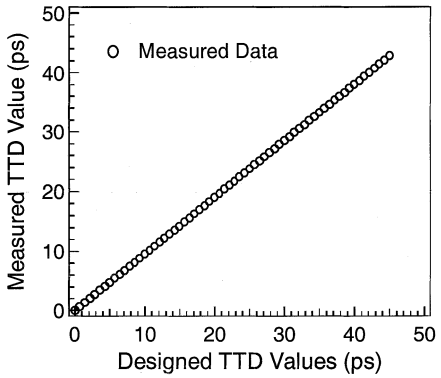

Fig. 5. Comparison between the measured absolute TTD and designed values.

input light, the interferometer output intensity can be expressed as

$$I_o = I_i \left[1 + m \cos\left(2\pi f \left(\Delta\tau_a - \tau_1\right)\right)\right] \tag{4}$$

where f is the optical frequency, m is the optical modulation index, $\Delta\tau_a$ is the absolute delay time defined in (3), and τ_1 is the absolute delay time in interferometer arm 1. The interferometer arm 1 is first adjusted so that the absolute delay in arm 1 is equal to the common path delay τ_0 of the tunable delay module. The adjustable part of the absolute time delay is then measured by counting the number of fringes over the specified optical frequency range at different binary switching states. Assuming there are M fringes over a bandwidth of Δf, the delay can be calculated as

$$\Delta\tau_a = \frac{M}{\Delta f}. \tag{5}$$

To improve measurement accuracy, we use an adjustable delay line to maintain the fringe number $M = 0$ on the optical spectrum analyzer. The absolute time delay was derived from the displacement change of the variable optical delay line. The measured data agrees well with the theoretical prediction, as shown in Fig. 5.

IV. First-Order PMD Emulation

The precise and repeatable DGD generation capability of our DGD module is ideal for generating a series of DGD values with any statistical distribution (e.g., Maxwellian, Gaussian, or Lorentz) for a given number of samples. We therefore developed the software tools necessary to control the DGD module so it can be used to generate statistical DGD samples with a Maxwellian distribution and a selectable average DGD value $\Delta\tau$. The tunable average DGD value for the Maxwellian distribution can be determined by using [21]

$$\sqrt{\frac{2}{\pi}}\frac{\Delta\tau^2}{\alpha^3}\exp\left[-\frac{\Delta\tau^2}{2\alpha^2}\right], \qquad \text{where } \alpha = \frac{\langle\Delta\tau\rangle}{\sqrt{\frac{8}{\pi}}}.$$

Fig. 6(a) shows the measured distribution for 500 samples with an average value of 10 ps, and Fig. 6(b) shows the instantaneous DGD of the samples. Although this is only first-order PMD emulation (almost no higher order effects involved), it has a much higher speed than a standard PMD emulator and can be precisely controlled. In addition, its features enable users to emulate pure or statistical all-order PMD distributions [22]–[24]. These characteristics should prove powerful in evaluating the dynamic performance of PMD compensators.

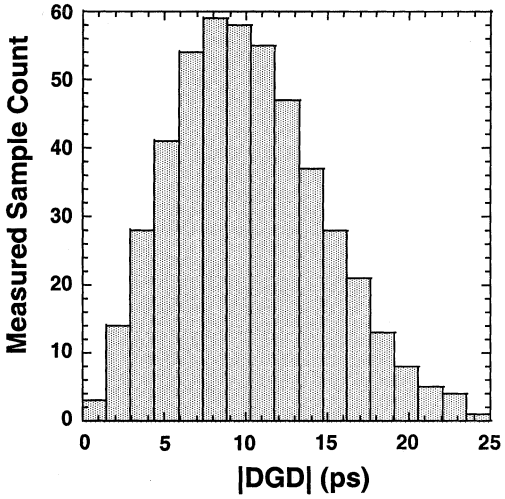

(a)

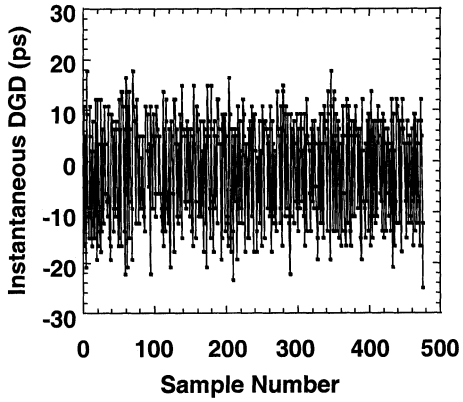

(b)

Fig. 6. Repeatable DGD generation is used to generate dynamic first-order PMD distribution with tunable average values. (a) First-order PMD distribution of 500 samples with an average DGD of 10 ps. (b) Instantaneous DGD values of the samples.

V. Dynamic Performance

In continuous data traffic network applications, it is critical that the system performance be unaffected during DGD state switching. Therefore, the dynamic performance of this DGD module must be well understood and controlled.

In our experiment, we first characterize the effect of switching on the DGD values. In principle, when the device is switched from one DGD state to another, the DGD value will change from one value to another precisely. However, because the device has a finite switching speed, the DGD value during switching is different than either the initial or final states. When the device is switched in smallest step $(2\delta\tau)$, the maximum DGD value excursion from the DGD value of the ending state is defined as the transient DGD. As it is difficult to directly measure the transient DGD during switching due to the limited response speed

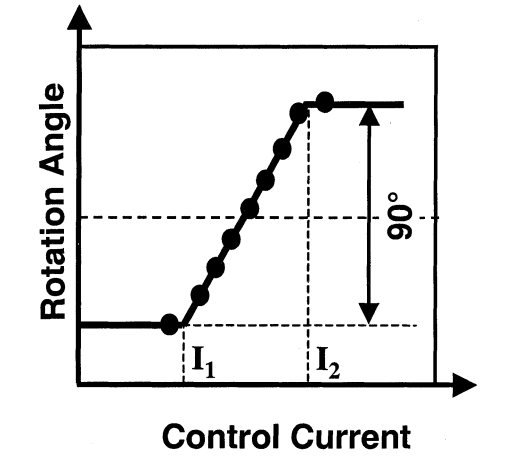

(a)

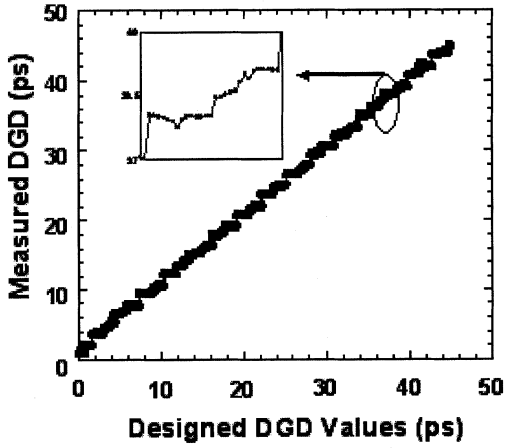

(b)

Fig. 7. Characterization of transient DGD effects during polarization switching. (a) Quasi-static measurement of transient DGD by step-varying the control current of the MO switches. (b) Measurement of transient DGD by equivalent small polarization variation between different DGD values from 0 to 45 ps.

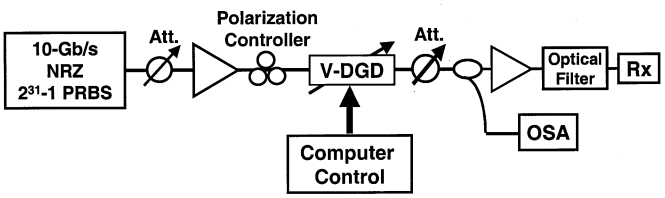

(a)

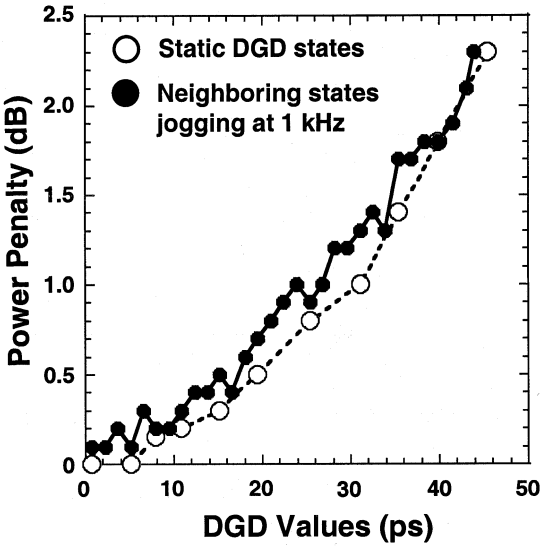

(b)

Fig. 8. System evaluation of the tunable DGD module. (a) Experimental setup of a 10-Gb/s NRZ ($2^{31}-1$ PRBS) link. (b) Measured power penalties for two cases. Open circle: the DGD module remains static after changing state. Solid circle: the DGD module keeps jogging back and forth between neighboring states at 1 kHz.

of the measurement instrument, we used a quasistatic measurement method. Instead of having a full 90° polarization rotation in one step to change the DGD value from one state to another, we incrementally change polarization rotation angles in steps of a few degrees [as shown in Fig. 7(a) by increasing or decreasing the control current on the MO switches] while measuring the corresponding DGD with a commercial polarization analyzer. We repeat the procedure for all DGD values from 0 to 45 ps in steps of 1.40 ps, with the results shown in Fig. 7(b). The insert shows the detailed DGD values between two adjacent DGD states. It is evident that the transient DGD is always less than the step size. The small transient DGD is critical when the device is used in PMD compensators. Note that there will also be second-order PMD involved during the switching. The value of second-order PMD can be up to several hundred ps^2, depending on the length (or DGD) of the crystals.

Another transient effect is the loss variation during fast polarization switching. Through proper mechanical alignment and electronic circuit design (e.g., proper arrangement of the switching sequence), this transient loss can be reduced to <0.6 dB, even in the case when all six bits are switched at the same time, while maintaining a total switching speed of less than 1 ms.

The most straightforward and effective evaluation of a fiber-optic device is to test the device in an actual fiber-optic link. In order to test the impact on a system due to the transient effects, we integrate the DGD element into a 10-Gb/s nonreturn-to-zero (NRZ) transmission link modulated at $2^{31}-1$ PRBS, as shown in Fig. 8(a). The input optical-signal-to-noise-ratio (OSNR) to the delay module is set to 30 dB (0.1-nm bandwidth) by changing the input power into the first erbium-doped fiber amplifier (EDFA). An optical preamplifier before the receiver is used to increase receiving sensitivity. The system's back-to-back sensitivity is measured to be -31 dBm. Power penalties are measured by comparing the receiver sensitivity of the system at a 10^{-9} BER with the back-to-back sensitivity. We measured two cases: 1) power penalties when the delay module is set at different static DGD values and 2) power penalties when neighboring states of the module are jogging back and forth at 1 kHz (1-ms continuous switching). As shown in Fig. 8(b), a negligible power penalty of <0.2 dB due to the fast polarization switching (jogging) was obtained. This result assures that the transient effects of the delay module will be too small to cause any concerns in a real system and that the device can be effectively used in systems for PMD compensation, emulation, or signal processing applications without causing harmful side effects.

We also measured the transient effect for the case in which there is no optical preamplifier before the receiver and found that the transient-induced power penalty is less than 0.5 dB when jogging at 1 kHz. Such a power penalty is mainly due to transient loss during switching.

VI. Applications

As mentioned in the introduction, the dynamic delay module presented in this paper has numerous applications in both fiber-optic communication systems and microwave systems.

A. High-Speed PMD Emulation

PMD emulation is important for evaluating systems' PMD susceptibility and for developing PMD compensators. A fast and repeatable DGD generator is particularly useful for testing the response time and effectiveness of a PMD compensator under different PMD varying conditions.

There are several approaches to making PMD emulators, such as those based on splitting the input light into two polarization components and delaying one of the components by free-space optics, those based on rotating the relative angles of several sections of birefringence crystals [25], and those based on heating or rotating different sections of polarization-maintaining (PM) fiber [26], [27]. All of these PMD emulators suffer from a slow response time (on the order of seconds) and poor repeatability, making them less effective in evaluating PMD compensators. In contrast, because of its high speed and precise DGD repeatability, the delay module reported in this paper is ideal for such applications. For example, our DGD module is capable of generating repeatable DGD variation as fast as 200 μs, and thus can be used for evaluating the impulse response of a PMD compensator that has a speed on the order of 1 ms.

B. First- and Higher Order PMD Compensation

As previously mentioned, a tunable DGD module is a key component in many PMD compensation configurations for first and higher order PMD [9]–[14]. In a recent demonstration of PMD compensation scheme, a variable DGD element is placed at the receiver to completely compensate the first-order PMD [10]. Some typical first-order and higher order PMD compensation schemes using a variable DGD module are shown in Fig. 9.

As a tunable DGD module based on polarization splitting and combining suffers from slow tuning speeds, as well as a large foot print and vibration sensitivity, it is not suitable for field deployment. Finally, the output polarization stability of such a device is poor due to the length fluctuations of the independent optical paths of the two polarization components. Such polarization instability complicates the PMD compensator feedback loop design and may cause the loop to be unstable.

On the other hand, the delay module reported in this paper has the advantage of compact size and high speed, making it field deployment friendly. In addition, its output polarization is much more stable than that of the DGD module described previously because here the two polarization components share the same optical path. Finally, the binary DGD tuning mechanism ensures that the module can be tuned to any desired DGD value precisely and quickly without any feedback control, eliminating the need of another DGD-control loop.

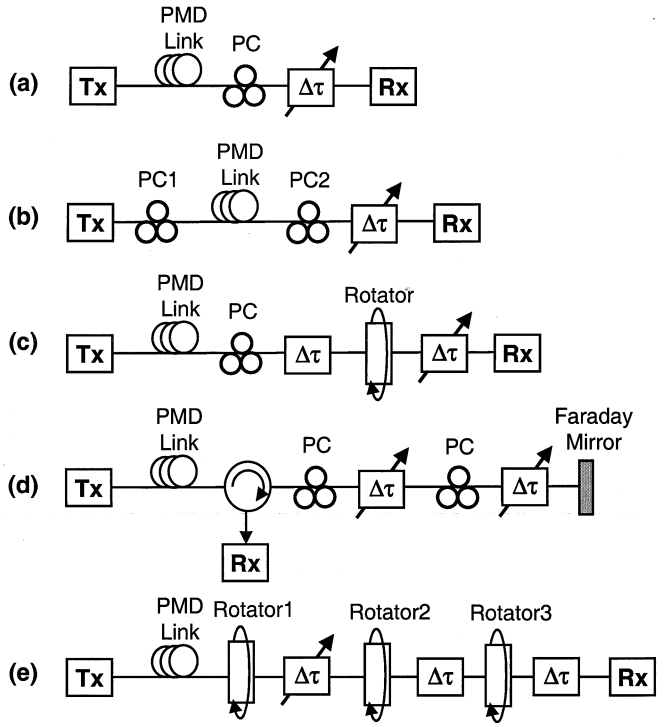

Fig. 9. Different approaches for PMD compensation using variable DGD modules. (a) [9]. (b) [10]. (c) [11]. (d) [12]. [13]. (e) [14].

C. Multiwavelength Laser Source With Tunable Channel Spacing

Multiwavelength lasers have received considerable attention recently due to their potential application to optical measurement, optical sensors, and wavelength-division-multiplexed systems. A PM fiber placed inside a ring laser cavity can function as a multiwavelength selector to produce a multichannel optical output [28], [29]. However, such line spacing is fixed once the length of the PM fiber is selected. To make a multiwavelength laser with tunable channel spacing, a tunable DGD module can be used. In principle, the channel spacing Δf is related to the DGD value of the module by Δf (Hz) $= 1/\mathrm{DGD}$ (ps). Experimental verification of this method using our variable DGD module is shown in Fig. 10 [30].

D. Bit Alignment in TDM Systems

In high-speed time-division-multiplexed (TDM) systems, it is critical to precisely position data in an assigned time slot at the transmission end and to select a desired time slot at the receiving end [16], [17]. As shown in Fig. 11, the delay module reported here can accomplish this function easily. Data from transmitter 1 (TX1) and transmitter 2 (TX2) are combined by a PBC before entering the variable DGD module. The signal from TX1 is aligned with one eigen-polarization axis of the device, and the signal from TX2 is aligned with the other. The relative group delay between the two signals can be delayed precisely and, thus, can align the data bits from the two transmitters in time.

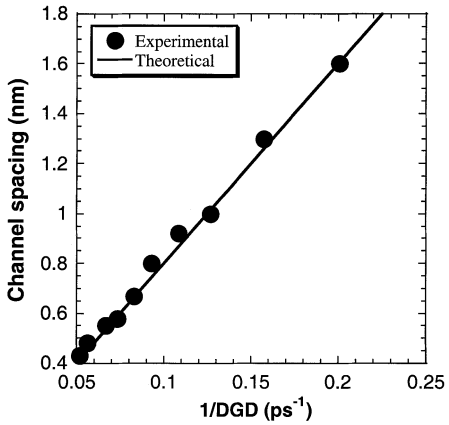

Fig. 10. Output channel spacing as a function of DGD for a multiwavelength fiber ring.

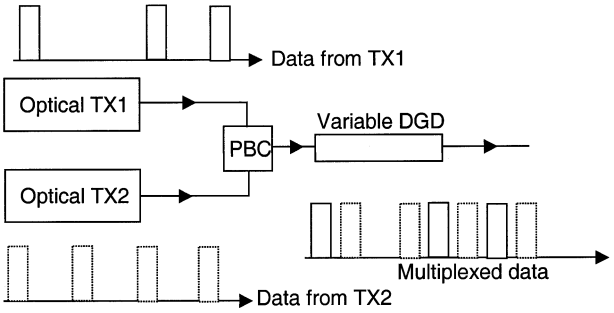

Fig. 11. Illustration of data bit alignment using the delay module described in this paper.

At the receiver side, the two channels can be demultiplexed via a PBS placed after a polarization stabilizer.

E. Beam Steering of Phased-Array Radar Systems

For airborne and space-based phased-array radar systems operating at millimeter-wave frequencies (20 GHz and above), fast beam steering with a fine scan resolution is required [31]. One effective method of steering the radar beam is to feed each radiation element on the radar panel with optical fibers and change the relative time delay of the signals feeding to the radiation elements, as shown in Fig. 12. As mentioned previously, the delay module reported in this paper can be used as a TTD for steering the phased-array radar [32]. This programmable TTD can be readily modified into a two-dimensional device and has the advantages of high packing density, low loss, and easy fabrication. The delay resolution of the device is sufficiently fine for accurate beam steering, and the total delay can be made adequately large by increasing the length of each crystal section to cover the desired scanning angles. This device can also be simplified to a phase-shifter/beam-former for phased arrays of narrow bandwidth, where true time delay is not necessary.

F. Transversal Filter

Fast and widely tunable filters are important for signal extraction and processing in spread spectrum microwave communication and radar systems [33]–[35]. Transversal filters based on photonics technology have several attractive features for such

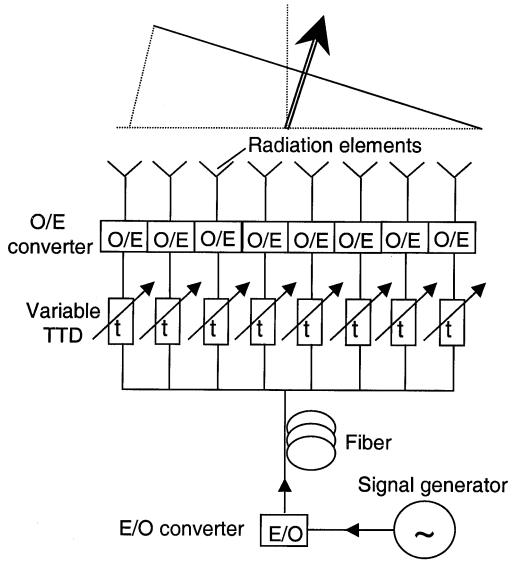

Fig. 12. Illustration of using the variable TTD module for steering a phased-array radar. The relative delays between the radiation elements are adjusted by the variable TTD to cause the total radiation wave front to tilt and hence effectively scan the angle of the radar beam.

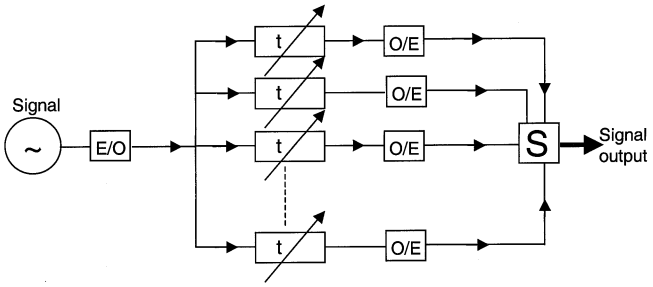

Fig. 13. Illustration of using the variable TTD module in a transversal filter. The output signal is the coherent summation of all branches. The relative phase (delay time) and amplitude changes in the branches alter the shape of the output signal.

applications, including wide bandwidth, high packing density, low loss, low weight, remote capability, and immunity to electromagnetic interference. True time delay is a critical element in a transversal filter, as shown in Fig. 13. The fast switching speed, high delay precision, and high delay repeatability of the delay module reported here are among the most attractive features for a transversal filter. These features in turn make the filter high speed, precise, and highly repeatable.

VII. Summary

In summary, we report the first realization of a high-speed variable delay module based on polarization switching. The device can either be used as a DGD module or a TTD module. Using a unique binary delay adjustment mechanism, this 6-bit device can precisely and repeatedly generate any DGD value from -45 to $+45$ ps with a resolution of 1.40 ps, or any TTD value from 0 to 45 ps with a resolution of 0.7 ps. The delay tuning speeds for both applications are under 1 ms and can be as fast as 0.1 ms. Devices with more crystal segments (i.e., bits) can be readily assembled based on the same design to either increase the delay range or improve the delay resolution. The

TABLE I
TYPICAL CHARACTERISTICS OF THE TUNABLE DGD MODULE

Parameter	Typical Value
Insertion loss	1.3±0.2 dB
PDL	< 0.28 dB
Switching time	< 1 ms
Optical return loss	>50 dB
TTD range	0~45 ps
DGD range	-45~45 ps
TTD resolution	0.7 ps
DGD resolution	1.40 ps
Transient loss	< 0.6 dB
Transient DGD	< 1.40 ps
WDL	< 0.15 dB
Switch voltage	TTL (5V)

delay range and the delay resolution of the current device as a variable DGD are designed for a 10-Gb/s network. They can be readily modified for a 40-Gb/s network by reducing the lengths of the birefringent crystals.

Due to the unique binary polarization switching design, the delay module also exhibits both excellent static and dynamic characteristics, as summarized in Table I. With a special emphasis on its dynamic figures of merit for PMD emulation and compensation applications, we demonstrated that the device exhibits a negligible transient-effect induced power penalty $(<0.2$ dB$)$ in a 10-Gb/s NRZ system.

REFERENCES

[1] C. D. Poole and J. Nagel, *Optical Fiber Telecommunications*. San Diego, CA: Academic, 1997, vol. III-A, ch. 6, pp. 114–161.

[2] H. Kogelnik, R. M. Jopson, and L. E. Nelson, *Optical Fiber Telecommunications*. San Diego, CA: Academic, 2002, vol. IV-B, ch. 15, pp. 725–861.

[3] H. Bülow, W. Baumert, H. Schmuck, F. Mohr, T. Schulz, F. Küppers, and W. Weiershausen, "Measurement of the maximum speed of PMD fluctuation in installed field fiber," in *Tech. Digest Optical Fiber Commun. Conf. (OFC'99)*, San Diego, CA, Feb. 1999, Paper WE4.

[4] Q. Yu and A. E. Willner, "Performance limits of first-order PMD compensators using fixed and variable DGD elements," *IEEE Photon. Technol. Lett.*, vol. 14, pp. 304–306, Mar. 2002.

[5] H. Rosenfeldt, C. Knothe, R. Ulrich, E. Brinkmeyer, U. Feiste, C. Schubert, J. Berger, R. Ludwig, H. G. Weber, and A. Ehrhardt, "Automatic PMD compensation at 40 Gbit/s and 80 Gbit/s using a 3-dimensional DOP evaluation for feedback," in *Tech. Dig. Optical Fiber Commun. Conf. (OFC'2001)*, Anaheim, CA, Mar. 2001, Paper PD27.

[6] P. C. Chou, J. M. Fini, and H. A. Haus, "Real-time principal state characterization for use in PMD compensators," *IEEE Photon. Technol. Lett.*, vol. 13, pp. 568–570, June 2001.

[7] L.-S. Yan, Q. Yu, A. B. Sahin, and A. E. Willner, "Differential group delay monitoring used as feed forward information for polarization mode dispersion compensation," *IEEE Photon. Technol. Lett.*, vol. 14, pp. 1463–1465, Oct. 2002.

[8] D. Sandel, F. Wüst, V. Mirvoda, and R. Noé, "Standard (NRZ 1×40 Gb/s, 210 km) and polarization multiplex (CS-RZ, 2×40 Gb/s, 212 km) transmissions with PMD compensation," *IEEE Photon. Technol. Lett.*, vol. 14, pp. 1181–1183, Aug. 2002.

[9] M. Karlsson, C. Xie, H. Sunnerud, and P. A. Andrekson, "Higher order polarization mode dispersion compensator with three degrees of freedom," in *Tech. Dig. Optical Fiber Commun. Conf. (OFC'2001)*, Anaheim, CA, Mar. 2001, Paper WO1.

[10] L.-S. Yan, Q. Yu, T. Luo, A. E. Willner, and X. S. Yao, "Compensation of higher-order polarization mode dispersion using phase modulation and polarization controller in the transmitter," *IEEE Photon. Technol. Lett.*, vol. 14, pp. 858–860, June 2002.

[11] Q. Yu, L.-S. Yan, Y. Xie, M. Hauer, and A. E. Willner, "Higher order polarization mode dispersion compensation using a fixed time delay followed by a variable time delay," *IEEE Photon. Technol. Lett.*, vol. 13, pp. 863–865, Aug. 2001.

[12] M. Shtaif, A. Mecozzi, M. Tur, and J. A. Nagel, "A compensator for the effects of high-order polarization mode dispersion in optical fibers," *IEEE Photon. Technol. Lett.*, vol. 12, pp. 434–436, Apr. 2000.

[13] N. Y. Kim, J. Park, H. Kim, and N. Park, "Second order PMD compensation using correlation factor between degree of polarization and depolarization rate," in *Tech. Dig. Optical Fiber Commun. Conf. (OFC'2002)*, Anaheim, CA, Mar. 2002, Paper WI6.

[14] P. B. Phua and H. A. Haus, "Deterministic approach to first- and second-order PMD compensation," *IEEE Photon. Technol. Lett.*, vol. 14, pp. 1270–1272, Sept. 2002.

[15] F. Heismann, D. A. Fishman, and D. L. Wilson, "Automatic compensation of first-order polarization mode dispersion in a 10 Gb/s transmission system," in *Proc. Eur. Conf. Optical Communication (ECOC'98)*, Madrid, Spain, 1998, pp. 529–530.

[16] S. Kawanishi, I. Shake, and K. Mori, "3 Tbits/s (160 Gbits $\times$ 19 ch) OTDM/WDM transmission experiment," in *Tech. Dig. Optical Fiber Communication Conf. (OFC'99)*, San Diego, CA, Feb. 1999, Paper PD-1.

[17] M. Nakazawa, "Solitons for breaking barriers to terabit/second WDM and OTDM transmission in the next millennium," *IEEE J. Select. Topics Quantum Electron.*, vol. 6, pp. 1332–1343, June 2000.

[18] W. Ng, A. Walston, G. Tangonan, J. J. Lee, I. Newberg, and N. Berstern, "The first demonstration of an optically steered microwave phased array antenna using true time delay," *J. Lightwave Technol.*, vol. 9, pp. 1124–1131, Sept. 1991.

[19] D. D. Dolfi, F. Michel-Gabriel, S. Bann, and J. P. Huignard, "Two-dimensional optical architecture for time delay beam forming in a phased array antenna," *Opt. Lett.*, vol. 16, pp. 255–257, 1991.

[20] X. S. Yao and L. Maleki, "A novel 2-D programmable photonic time-delay device for millimeter-wave signal processing applications," *IEEE Photon. Technol. Lett.*, vol. 6, pp. 1463–1465, Dec. 1994.

[21] C. D. Poole, J. H. Winters, and J. A. Nagel, "Dynamical equation for polarization dispersion," *Opt. Lett.*, vol. 16, no. 6, pp. 372–374, 1991.

[22] L. Möller, J. H. Sinsky, H. Haunstein, S. Chandrasekhar, C. R. Doerr, J. Leuthod, C. A. Burrus, and L. L. Buhl, "Novel higher order PMD distortion mitigation technique for RZ signals," in *Tech. Dig. Optical Fiber Commun. Conf. (OFC'2002)*, Anaheim, CA, Mar. 2002, Paper WI5.

[23] J. H. Lee and Y. C. Chung, "Statistical PMD emulator using variable DGD elements," in *Tech. Dig. Optical Fiber Commun. Conf. (OFC'2002)*, Anaheim, CA, Mar. 2002, Paper ThA4.

[24] P. B. Phua and H. A. Haus, "A deterministically controlled four-segment polarization-mode dispersion emulator," *J. Lightwave Technol.*, vol. 20, pp. 1132–1140, July 2002.

[25] J. N. Damask, "A programmable polarization-mode dispersion emulator for systematic testing of 10 Gb/s PMD compensators," in *Tech. Dig. Optical Fiber Commun. Conf. (OFC'2000)*, Baltimore, MD, Mar. 2000, Paper ThB3.

[26] R. Khosravani, I. T. Lima Jr, P. Ebrahimi, E. Ibragimov, A. E. Willner, and C. R. Menyuk, "Time and frequency domain characteristics of polarization-mode dispersion emulators," *IEEE Photon. Technol. Lett.*, vol. 13, pp. 127–129, Feb. 2001.

[27] M. C. Hauer, Q. Yu, A. E. Willner, E. R. Lyons, C. H. Lin, A. A. Au, and H. P. Lee, "Compact, all-fiber PMD emulator using an integrated series of thin-film micro-heaters," in *Tech. Dig. Optical Fiber Commun. Conf. (OFC'2002)*, Anaheim, CA, Mar. 2002, Paper ThA3.

[28] N. Park and P. F. Wysocki, "24-line multiwavelength operation of erbium-doped fiber-ring laser," *IEEE Photon. Technol. Lett.*, vol. 8, pp. 1459–1461, Nov. 1996.

[29] S. Yamashita and T. Baba, "Spacing-tunable multiwavelength fiber laser," *Electron. Lett.*, vol. 37, no. 16, pp. 1015–1017, 2001.
[30] T. Luo, L.-S. Yan, Y. Q. Shi, Z. Pan, Y. W. Song, A. E. Willner, and X. S. Yao, "Dynamically tunable wavelength spacing multi-wavelength ring laser using a programmable DGD module as the intra-cavity filter," in *Tech. Dig. Conf. Lasers Electro-Optics (CLEO'2003),* Paper CMY1, Baltimore, MD, June 2003.
[31] R. Tang and R. W. Burns, *Phased Arrays in Antenna Engineering Handbook*, 3rd ed, R. C. Johnson, Ed. New York: McGraw-Hill, 1992, ch. 20.
[32] E. Toughlian and H. Zmuda, "A photonic variable RF delay line for phased array antennas," *J. Lightwave Technol.*, vol. 8, pp. 1824–1828, Dec. 1990.
[33] D. Nortton, S. Johns, and R. Soref, "Tunable wideband wicrowave transversal filter using high dispersive fiber delay lines," in *Proc.4th Biennial Dept. Defense Fiber Optics Photonics Conf.*, Maclean, VA, 1994, pp. 297–301.
[34] B. Moslehi, K. Chau, and J. Goodman, "Fiber-optic signal processors with optical gain and reconfigurable weights," in *Proc. 4th Biennial Dept. Defense Fiber Optics Photonics Conf.*, Maclean, VA, 1994, pp. 303–309.
[35] H. Zmuda and E. Toughlian, "Adaptive microwave signal processing: A photonic solution," *Microwave J.*, pp. 58–71, Feb. 1992.

Lianshan Yan (S'99) was born in Shandong, China, in 1971. He received the B.E. degree in optical engineering from Zhejiang University, Hangzhou, China, in 1994, and is currently working toward the Ph.D. degree in electrical engineering at the University of Southern California (USC), Los Angeles.

From 1994 to 1999, he was working on solid-state lasers at North China Research Institute of Electro-Optics. He joined the Optical Communications Laboratory (OCLAB), USC, in September 1999. He is also a Part-Time Engineer with the General Photonics Corporation, Los Angeles, CA. His main research interests are enabling technologies for long-haul wavelength-division-multiplexing (WDM) systems and polarization effects in fiber transmission. He is the author and coauthor of more than 50 papers in international journals and conference proceedings.

Mr. Yan is a Student Member of the IEEE Lasers and Electro-Optics Society (LEOS), the IEEE Communications Society, and the Optical Society of America (OSA). He is one of the recipients of LEOS Graduate Fellowship in 2002.

C. Yeh, photograph and biography not available at the time of publication.

G. Yang, photograph and biography not available at the time of publication.

L. Lin, photograph and biography not available at the time of publication.

Z. Chen, photograph and biography not available at the time of publication.

Y. Q. Shi, photograph and biography not available at the time of publication.

Alan Eli Willner (S'87–M'88–SM'93) received the B.A. degree from Yeshiva University, New York, NY, and the Ph.D. degree in electrical engineering from Columbia University, New York, NY.

He has worked at AT&T Bell Laboratories and Bellcore and is Professor of Electrical Engineering at the University of Southern California, Los Angeles. He has more than 400 publications, including one book. His research is in optical fiber communication systems.

Dr. Willner is a Fellow of Optical Society of America (OSA) and was a Fellow of the Semiconductor Research Corporation. His activities have included Vice-President for Technical Affairs for IEEE Lasers and Electro-Optics Society (LEOS); Elected Member of the IEEE LEOS Board of Governors; Co-Chair of the Optical Society of America (OSA) Science and Engineering Council; Photonics Division Chair of the OSA; General Chair of the IEEE LEOS Annual Meeting; Program Co-Chair of the OSA Annual Meeting; Program Co-Chair of CLEO; Steering and Technical Committee of the OFC, Program Committee Member of ECOC; Editor-in-Chief of the JOURNAL OF LIGHTWAVE TECHNOLOGY (*JLT*); Editor-in-Chief of the IEEE JOURNAL OF SELECTED TOPICS IN QUANTUM ELECTRONICS; Guest Editor of the *JLT* Special Issue on Wavelength-Division Multiplexing (WDM); and Guest Editor of the IEEE JOURNAL OF QUANTUM ELECTRONICS. He has received the NSF Presidential Faculty Fellows Award from the White House, the David and Lucile Packard Foundation Fellowship, the National Science Foundation National Young Investigator Award, the Fulbright Foundation Senior Scholar Award; the IEEE LEOS Distinguished Lecturer Award, the USC/Northrop Outstanding Junior Engineering Faculty Research Award, the USC/TRW Best Engineering Teacher Award, and the Armstrong Foundation Memorial Prize.

X. Steve Yao received the M.S. and Ph.D degrees in electrical engineering/electrophysics from the University of Southern California in 1989 and in 1992, respectively.

He is the founder, president, and CEO of General Photonics Corporation. He was with NASA's Jet Propulsion Laboratory (JPL) from 1990 to 2000, concentrated on the research and development of microwave photonic devices and systems, where he invented the optoelectronic oscillator for generating the world cleanest 10–80 GHz signals. He was responsible for the design and demonstration of the X-band fiber optic antenna remoting system for NASA's Deep Space Network. His innovative phase-compensated fiber optic link design was successfully implemented in NASA's SRTM mission and is instrumental for the high resolution of the three-dimensional mapping of the Earth from space. Prior to JPL, he was an Optical Engineer at ADC Fiber Optics (a division of ADC Telecommunications) from 1985 to 1987, where he was responsible for developing the first generation of fiber optic WDM devices. He has authored more than 25 journal publications and given invited speeches in numerous major photonics-related conferences. He also contributed a book chapter in radio frequency photonic technology in optical fiber links, detailing his breakthrough research in optoelectronic oscillators for generating 10-GHz and higher frequency signals. He holds 20 U.S.-issued patents, 15 pending applications, and 25 NASA innovation awards.

Dr. Yao also served as a Member of the Technical Committee in the Optical Fiber Communications conferences (OFC) for three terms (1998, 2000, and 2001). He was the organization Committee Member for the Microwave Photonics Conference in 2000 (MWP '00).